Surface Science 653 (2016) 130–137

Contents lists available at ScienceDirect

Surface Science

journal homepage: www.elsevier.com/locate/susc

Dehydrocyclization of peripheral alkyl groups in porphyrins at Cu(100) and Ag(111) surfaces

Christopher G. Williams [a], Miao Wang [b], Daniel Skomski [a], Christopher D. Tempas [a], Larry L. Kesmodel [b], Steven L. Tait [a,b,*]

[a] Dept. of Chemistry, Indiana University, Bloomington, IN, USA
[b] Dept. of Physics, Indiana University, Bloomington, IN, USA

ARTICLE INFO

Article history:
Received 12 May 2016
Accepted 22 June 2016
Available online 29 June 2016

Keywords:
Dehydrocyclization
Dehydrogenation catalysis
Surface functionalization
Organic adsorbates
High-resolution electron energy loss spectroscopy
Scanning tunneling microscopy

ABSTRACT

The self-assembly of organic and metal-organic species at metal surfaces is a topic of high interest for applications that can benefit from tunable surface functionalization through organic building block design. As the complexity of molecular building blocks increases to direct ordering and function, thermal stability of the adsorbate often increases opening up new surface-catalyzed reaction pathways. We report dehydrocyclization of octaethylporphyrin to tetrabenzoporphyrin on the Cu(100) and Ag(111) surfaces at 500–600 K. Dehydrocyclization of smaller species is not typically observed on these surfaces at low pressure due to short adsorption lifetimes. The dehydrocyclization of peripheral ethyl groups forms benzo groups which then undergo additional dehydrogenation. The reaction products are characterized by high resolution electron energy loss spectroscopy (HREELS), scanning tunneling microscopy (STM), and X-ray photoelectron spectroscopy (XPS). These results extend our understanding of reaction pathways that may be encountered as molecular building blocks increase in size and complexity on relatively inert surfaces.

© 2016 Elsevier B.V. All rights reserved.

1. Introduction

Surface patterning with organic molecules is a strategy of growing interest to develop electronic [1,2] and catalytic chemical functions [3] in organic thin films [4]. Porphyrin molecules, such as those studied here, are often used in optical adsorption films [5,6] or thin film electronics [7]. Many of these potential applications benefit from excellent ordering and chemical fidelity during film formation [8]. Structural organization has been directed by covalent interactions [9], metal-organic coordination [10], electrostatic interactions [11], hydrogen-bonding interactions [12], or van der Waals (vdW) contacts [13–15].

Studies of surface patterning and functionalization by tailored organic molecules often employ relatively inert surfaces, such as Au, Ag, Cu, and graphite. As larger and more complex molecules are developed for surface functionalization, the thermal adsorption stability increases and new surface-catalyzed reaction pathways need to be considered as these may impact short-term and long-term performance of these layers. Here, we study the dehydrocyclization of ethyl-functionalized porphyrin molecules on Cu(100) and Ag(111) surfaces upon annealing to 500–600 K (Scheme 1).

Dehydrogenation of alkane chains occurs at high temperature in the gas phase (~750–1150 K) and so the reaction is typically performed in the presence of a solid catalyst [16], commonly Pt or PtSn alloys, in the temperature range of 300–500 K [17]. Dehydrocyclization reactions, a subset of dehydrogenation reactions that involve the further step of ring formation, are of high interest for the oil refining industry as a method to increase the octane number of fuels [18]. Dehydrocyclization requires high temperature (873 K for 1,3-pentadiene to cyclopentadiene [19]) or a catalyst, such as Ir or Ru complexes [20,21]; zeolite materials loaded with Co, Pt, Cu, Zn, Ga, or In metals [22–24]; or on Rh, Ir, Ni, Pd, Pt, Cu_3Pt, or W carbide surfaces [25–36]. Most of the dehydrocyclization surface studies rely on surfaces that can catalyze the reaction at a temperature below thermal desorption [37–39]. Single crystal surfaces of Cu, Ag, and Au are typically considered inert for this reaction because of the low desorption temperature (<300 K) of small molecule species ($\leq C_{10}$) of alkanes, alkenes, alkynes, cyclohexanes, and cyclohexenes [40–43]. Substituted benzene rings such as styrene [44,45], phenylacetylene [46], 1-phenyl-1-propyne [47], and naphthalene [48,49] also desorb from Cu and Ag surfaces at lower temperatures (<400 K). These relatively inert surfaces only become active for dehydrocyclization at high pressure and high temperature [19,50,51]. There have been several examples of cyclodehydrogenation of aromatic rings on Cu(111) or Pt(111) [52,53], including some that formed more extended polyaromatic structures [54–57]. Previous dehydrocyclization studies of alkane substituted porphyrins used Fe-OEP, which was

* Corresponding author at: Dept. of Chemistry, Indiana University, Bloomington, IN, USA.
E-mail address: tait@indiana.edu (S.L. Tait).

http://dx.doi.org/10.1016/j.susc.2016.06.013
0039-6028/© 2016 Elsevier B.V. All rights reserved.

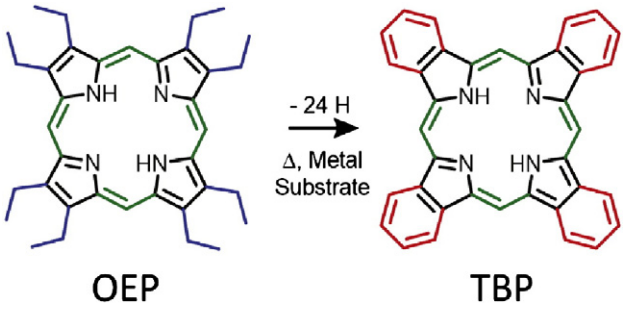

Scheme 1. Dehydrocyclization of octaethylporphyrin (OEP) to tetrabenzoporphyrin (TBP).

characterized through Kondo resonance and scanning tunneling microscopy (STM) on Cu(111) and Au(111) [58,59]. In these studies, porphyrin molecules were stable on the surface up to temperatures of 430 K on Cu(111) and 530 K on Au(111) where dehydrocyclization of the alkanes took place. More recently, ethyl-substituted phthalocyanines have been shown to form polymeric surface structures or monomers with closed rings by dehydrogenation on Au(111) [60]. To the best of our knowledge, no vibrational surface studies have shown dehydrocyclization on Cu(100) or Ag(111) surfaces.

This study provides spectroscopic evidence for dehydrocyclization of alkane substituents on porphyrin molecules, catalyzed by Ag and Cu surfaces. We report dehydrocyclization of peripheral ethyl groups on octaethylporphyrins (OEP) on Cu and Ag surfaces. Beyond the dehydrocyclization reaction, we observe an additional dehydrogenation step. We additionally found that this dehydrocyclization reaction is sensitive to the metal substrate utilized, but is insensitive to Pt metallation within the ring.

2. Experimental

OEP and TBP were purchased from Frontier Scientific (>95% purity) and Pt-OEP was purchased from Sigma Aldrich (98% purity). Each was degassed in ultra-high vacuum (UHV) overnight for further purification (OEP and Pt-OEP at 410 K and TBP at 520 K). OEP and Pt-OEP were deposited at 490 K and TBP at 620 K from a Knudsen-type evaporator to achieve a deposition rate of about 0.1 monolayers per minute, as monitored by quartz crystal microbalance (QCM). The surface coverage was verified using Auger electron spectroscopy (AES), where the full monolayer (1.0 ML) is calibrated by observing a slope change in AES intensity *vs.* deposition time upon monolayer completion and initiation of the second layer. In the studies presented here, we used a surface coverage of about 0.75 ML.

In each experiment, a Cu(100) or Ag(111) surface was cleaned by cycles of 1.5 keV Ar^+ sputtering followed by thermal annealing at 730 K. Clean surfaces were indicated by low diffuse background intensity and high metal to carbon signal ratio in Auger spectra and sharp low energy electron diffraction (LEED) patterns. The surface was cooled gradually to 320 K before deposition. Organic deposition was done in a separate but connected UHV chamber. Sample surface temperature was monitored by a thermocouple attached to the back side of the sample stage, which had been previously calibrated to the surface temperature. Incremental annealing experiments were conducted with 15 minute annealing time at each temperature.

All HREELS experiments were performed with a double-pass 127° angle cylindrical deflection electron spectrometer (LK Technologies, model LK 2000) operated at an initial beam energy of 10 eV and a peak width of 58 ± 6 cm^{-1}.

The scanning probe microscopy (SPM) system is equipped with both STM (SPM UHV 750, RHK Technologies) as well as X-ray photoelectron spectroscopy (XPS) (electron energy analyzer PHOIBOS 150 and Mg/Al dual anode X-ray source XR-50, SPECS GmbH). The interconnected vacuum chambers allow for STM and XPS on the same samples without exposure to air. STM imaging and XPS acquisition were conducted at room temperature. The well-characterized, (3 × 3) structure of terephthalic acid on the Cu(100) surface [61–63] was used to calibrate the SPM instrument. Sharp tungsten STM tips were fabricated with electrochemical etching. Bias voltages of 1.0 to 1.2 V and set point currents from 0.2 to 0.4 nA were generally used for the STM imaging. STM image analysis was conducted using the WSxM software [64].

3. Results and discussion

3.1. Adsorption of OEP and Pt-OEP on Cu(100) and on Ag(111)

OEP and Pt-OEP were each studied by HREELS on each of two surfaces: Cu(100) and Ag(111). In each experiment, 0.75 ML of one of the molecules was deposited to the surface while the surface was held at room temperature. HREEL spectra for each of these four experiments are shown in Fig. 1. The spectra were normalized by the average intensity of the flat background between 2220 and 2460 cm^{-1} to account for differences in initial beam current. Peak assignments were made by comparison to prior vibrational spectroscopy studies of porphyrins [65–67] and are summarized in Table 1.

The features in the HREEL spectra can be organized into five regions (Figs. 1 and 2 and Table 1) based on assignments made in previous studies of related systems [65,67] and on DFT calculations of vibrational spectra [68]. The peaks at 347, 435, 632, and 779 cm^{-1} are out-of-plane deformations of the porphyrin ring [65,67] (peak energies in this paragraph are for OEP/Cu(100), others are listed in Table 1). The peaks at 955 and 1028 cm^{-1} are rocking vibrational modes of the ethyl groups [65,67]. In-plane deformation modes are observed at 1120 and 1180 cm^{-1}. The ethyl C—C stretching modes were assigned to the three peaks at 1307, 1365, and 1432 cm^{-1}. C—H stretching modes account for the features in the range 2900–3100 cm^{-1}. Our experiments indicate two sets of C—H stretching modes. The more intense set is due to the ethyl C—H stretch (2846 and 2912 cm^{-1}). The other C—H feature is a shoulder on the high energy side of the peak (~3100 cm^{-1}), which is due to the C—H stretch at the methine C on the side of the ring. The latter is expected to shift to higher energy (above 3100 cm^{-1}, as in Fig. 2) upon metallation of the porphyrin [65].

In STM images OEP on Cu(100) appears as single lobes that do not exhibit long range ordering (Fig. 3A). On Ag(111), OEP molecules also appear as single lobes, but do order at room temperature (Fig. 3B) and match the unit cell measurements ($a = 1.55 \pm 0.10$ nm, $b = 1.45 \pm$

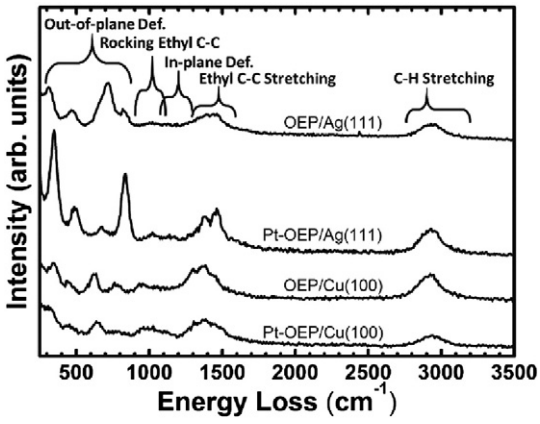

Fig. 1. Room temperature HREEL spectra for OEP and Pt-OEP molecules on both the Cu(100) and Ag(111) surfaces. Note that the out-of-plane deformation (def.) modes below 1000 cm^{-1} for OEP/Cu are more similar to either Pt-OEP spectrum than to OEP/Ag indicating that OEP likely undergoes self-metallation at room temperature on Cu(100) to Cu-OEP, but not on Ag(111). Peak assignments are presented in Table 1 and discussed in the text.

Table 1
Comparison of HREELS features of various OEP molecules and previous solution and thin film OEP studies.

	H_2-OEP (Cu-OEP) Cu(100) (cm^{-1})	H_2-OEP Ag(111) (cm^{-1})	Pt-OEP Cu(100) (cm^{-1})	Pt-OEP Ag(111) (cm^{-1})	Solution IR Cu-OEP [65] (cm^{-1})	Solution IR Ni-OEP [65] (cm^{-1})	Solution IR H_2-OEP [65] (cm^{-1})	RAIRS Ni-OEP [67] (cm^{-1})
Out-of-plane porphyrin ring deformation	347	311	297	348	336	355	328	
	435	457	447	487	443	475	475	
	632	713	649	670	717	713	720	
	779	825	(788)	831	750	754	745	710
Ethyl rocking	(955)		(975)		954	954	950	753
	(1028)	(1014)		(1029)	1018	1018	1014	954
In-plane porphyrin ring			(1096)		1058	1054	1057	1019
	(1120)	(1124)	(1147)	(1147)	1148	1147	1147	
					1271	1272	1277	
Ethyl C—C stretching	1307	1307	1324	1330	1370	1372	1370	
	1365	1374	1379	1375	1381	1385	1397	1367
	1432	1447	1452	1455	1452	1453	1450	
Ethyl C—H	2846	2833	2820	2827	2875	2872	2875	2868
					2935	2935	2938	2928
	2912	2930	2930	2929	2965	2965	2970	2962
Porphyrin ring C—H	(3103)	(3076)	(3119)	(3112)	3123	3185		

0.10 nm) reported in a previous STM study [69]. A lack of ordering of OEP on Cu(111) was previously attributed to N-Cu interaction [70], which effectively pins the molecules to the surface and limits their diffusivity.

Comparing HREELS features for OEP and Pt-OEP on two different surfaces (Fig. 1 and Table 1) reveals a few notable differences. All of the ring deformation modes on Cu(100) are at lower energies than on Ag(111), possibly due to stronger molecule-surface interactions taking place with the Cu(100) surface that soften intramolecular bonding. The intensities of the C—H stretch modes are similar for the four spectra in Fig. 1, consistent with our estimation of similar surface coverage in each experiment. The ring deformation mode at 831 cm^{-1} for Pt-OEP/Ag(111) is much more intense than for the other systems studied. There is significant variation in the intensities of out-of-plane porphyrin ring modes, likely due to differences in local adsorption site, *i.e.*, local electron distribution on the surfaces which differ in structure and packing symmetry [71–75].

Some of this difference may also be due to metallation (note that OEP and Pt-OEP are quite similar on Cu). It has been demonstrated that protoporphyrin undergoes spontaneous metal coordination (metallation) at room temperature on Cu(100) and Cu(110) surfaces [76] and that tetraphenyl porphyrin (TPP) does the same on a Cu(100) surface between 285 and 450 K [77]. Metallation is also indicated in our experiments by the position and intensity of the out-of-plane mode which is below 670 cm^{-1} for each of the metallated species. For example, this peak is observed at 632 cm^{-1} for Cu-OEP/Cu(100), while it appears at 713 cm^{-1} with much higher intensity for the non-

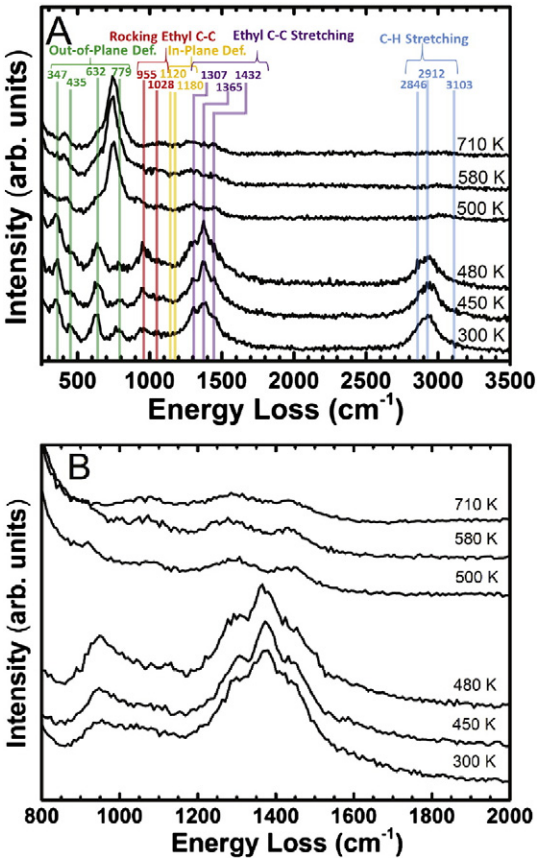

Fig. 2. (A) HREEL spectra of OEP (metallated to Cu-OEP) on Cu(100) after annealing incrementally up to 710 K for 15 min at each temperature. Each spectrum was recorded after cooling the sample to room temperature. Major spectroscopic changes after annealing to 500 K include an increase to C—H bending (735 cm^{-1}), decrease to the ethyl rocking and stretching modes (close-up in B, 5× scaling relative to A), and a significant decrease in the C—H region.

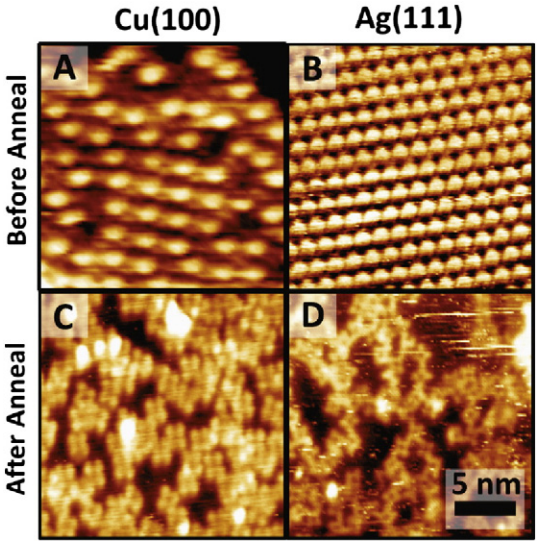

Fig. 3. STM images of OEP (A, C) on Cu(100) and (B, D) on Ag(111) (A, B) before and (C, D) after annealing above 600 K. (A, B) Before dehydrocyclization, OEP appears in STM as a single-lobed feature. (C, D) After annealing above the dehydrocyclization temperature, the OEP has converted to TBP and appears as a four-fold symmetric structure. Scale bar in the lower right applies to all four images. Images were recorded at room temperature (A, B) without annealing or after annealing to (C) 610 K or (D) 710 K. STM bias 1.0–1.2 V, setpoint current 0.2–0.4 nA.

metallated OEP/Ag(111) (Fig. 1 and Table 1). Self-metallation of OEP at room temperature on Cu(100) [76], but not on Ag(111) [78], is consistent with prior studies. OEP on Ag(111) does not show indications of metallation until temperatures well above dehydrocyclization temperature, approximately 700 K, as evidenced by XPS (Fig. S8). We also observed a new HREELS feature at 113 cm^{-1} (Fig. S9), which was assigned to metal-N bond formation resulting from self-metallation. Because of its proximity to the large elastic scattering feature, that feature is somewhat difficult to distinguish on Ag(111) and could not be conclusively resolved for experiments on Cu(100).

3.2. Dehydrocyclization of OEP on Cu(100) and on Ag(111)

After heating OEP on Cu(100) to 500 K, significant spectral changes are observed (see Fig. 2 and Table 2). New ring deformation modes emerge around 1300 cm^{-1} and a significant new feature is observed at 735 cm^{-1}, which is assigned as the out-of-plane C—H bending mode on an aromatic system [79]. Ethyl C—C stretches (1350 cm^{-1}) and ethyl C—H rocking and stretching modes that were present before annealing are no longer observed after annealing. The spectrum matches very well with a previously reported HREELS study of Cu-phthalocyanine (Cu-Pc) and other Pc molecules [79–82]; note that phthalocyanine is nearly identical to TBP other than the methine C in TBP (green in Scheme 1) being replaced by N in phthalocyanine. These changes, taken together, indicate a chemical transformation of the peripheral ethyl groups to aromatic benzo groups, *i.e.*, a dehydrocyclization (Scheme 1). The temperature of 500 K is consistent with other studies of dehydrogenation of ethyl groups and C—H bond scission on Cu and other surfaces [59,83]. The dehydrocyclization of OEP on Cu(100) at 500 K (15 minute anneal) (Fig. 2) is higher in temperature than a previous report for the dehydrocyclization of Fe-OEP on Cu(111) at 430 K (60 minute anneal) [59].

Most of the intensity of the C—H stretching feature is lost upon dehydrocyclization. The small remnant of this peak is likely due to hydrogen on the benzo groups (red carbons after dehydrocyclization reaction in Scheme 1) and the four porphyrin methine C—H bonds (green carbon in Scheme 1); these may all be weak HREELS signals because of their orientation parallel to the surface. The C—H position after dehydrocyclization is above 3000 cm^{-1}, *i.e.*, the remaining C—H bonds on the porphyrin core are stronger than the ethyl C—H before dehydrocyclization, as expected [65].

Dehydrocyclization of OEP takes place 100 K higher on the Ag(111) surface (600 K) than on the Cu(100) surface (500 K) (compare Figs. 2 and 4). It has been demonstrated that porphyrins will self-metallate on the Cu(100) surface at room temperature [76], so we investigated whether the reaction temperature differences were due to metallation of the porphyrin rather than inherent differences in surface reactivity. We found that the dehydrocyclization of Pt-OEP occurs at the same temperature as OEP on Cu(100) (Figs. 2 and 4C) and on Ag(111) (Fig. 4A and B).

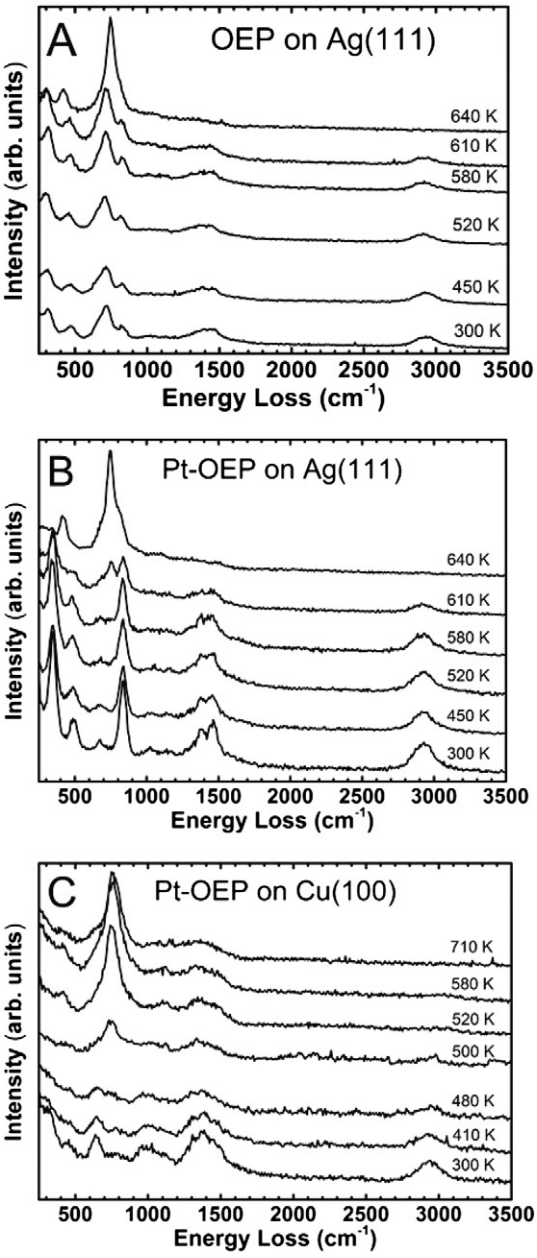

Fig. 4. Annealing of Cu(100) and Ag(111) surfaces with 0.75 ML OEP and Pt-OEP adlayers. Data for OEP on Cu(100) can be found in Fig. 2. Dehydrocyclization observed at (A) 640 K for OEP/Ag(111), (B) 610 K for Pt-OEP/Ag(111), (C) 500 K for Pt-OEP/Cu(100),and (Fig. 2) 500 K for OEP/Cu(100).

Table 2
HREELS vibrational data for the analysis of the dehydrocyclized OEP molecules.

	Surface formed H_2-TBP (Cu-TBP) Cu(100) (cm^{-1})	Surface formed H_2-TBP Ag(111) (cm^{-1})	Surface formed Pt-TBP Cu(100) (cm^{-1})	Surface formed Pt-TBP Ag(111) (cm^{-1})	TBP Cu(100) (cm^{-1})	TBP Ag(111) (cm^{-1})	708 K annealed TBP Cu(100) (cm^{-1})	708 K annealed TBP Ag(111) (cm^{-1})	HREELS Cu-Pc [79] (cm^{-1})
		297		295	296	308	282	304	282
Out-of-plane deformation	398	414	404	413	436	425	421	421	443
	640	626	634	655	641	(678)	641	(678)	
Out-of-plane bending C—H	735	751	756	743	759	741	751	751	726
									766
					941				
In-plane stretching C—C, C—N	1073	1074	1107	1102	1043		1065		1100
In-plane double bond stretching	1271	1324	1350	1322	1373	1359	1315	1322	1340
	1424	1477	1459	1476	1425	1432	1432	1513	1460
C—H stretching					2921	2900			
	3022		3062		3009	3031	3046	3046	3080

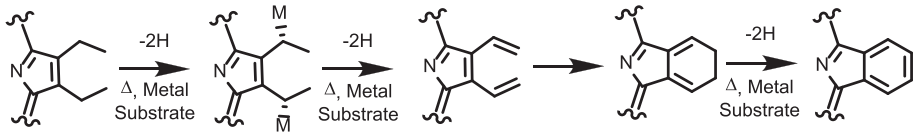

Scheme 2. Proposed mechanism for the dehydrocyclization of ethyl groups on OEP.

The temperature of dehydrocyclization on Ag(111) at 600 K is higher than measurements on the (111) surfaces of metals in the same group; dehydrocyclization has been reported for Fe-OEP on Cu(111) at 430 K [59] and for H_2-OEP on Au(111) at 530 K [58]. Dehydrocyclization on each of those surfaces occurs at significantly higher temperatures than on Pt(111) (300 K) [31] or on Cu_3Pt(111) (393 K) [26,29,30].

The possibility of porphyrin decomposition was excluded because the annealing temperatures employed here (500–710 K) are comparable to other studies of intact porphyrins on similar surfaces [83] and are too low to expect a full decomposition of the molecule to a graphitic layer (>1100 K) [84]. The HREEL spectra measured after annealing above 500 K do not resemble HREEL spectra of graphene as our spectra lacked the very broad peak features at the specular angle characteristic to graphene surface plasmons [85,86]. While there is the possibility that the molecule is decomposing to smaller molecules other than graphene, the peaks located within the 900–1500 cm^{-1} region are similar to the peaks within HREELS of phthalocyanine and cobalt protoporphyrin IX (Co-PP) [66,79]. The HREELS spectra share the same 1080, 1244, 1429 cm^{-1} peak structure (see Fig. 2B) of the Co-PP which are from porphyrin ring bending, breathing, and C—H wagging. AES C, XPS C 1*s*, and XPS N 1*s* analysis before and after annealing show less than 5% loss of signal, so no significant desorption occurred at 500 K.

STM imaging before (Fig. 3A and B) and after (Fig. 3C and D) annealing above 600 K shows a significant structural change that also indicates dehydrocyclization. Before annealing, OEP molecules are imaged as single lobes on each surface. After annealing above 600 K, each OEP molecule is imaged in STM as a four-lobe structure on either surface. The distance between diagonal lobes is 1.1 nm (Fig. S11), consistent with the positions of opposite benzo groups in TBP.

It is likely that the dehydrocyclization mechanism here is similar to that derived for hexenes on a Cu_3Pt surface [25,30]. The first dehydrogenation on the ethyl group is likely at the more acidic allylic α carbon hydrogen. The subsequent dehydrogenation of the β carbon forms the vinyl species, which then undergoes a 6π pericyclic rearrangement, followed by further dehydrogenation to form the benzo group (Scheme 2). Normally, alkane/alkene C—C bond formation is significantly slower than further dehydrogenation [37], but the positioning of the two ethyl groups in neighboring positions on the porphyrin ring may favor cyclization over further dehydrogenation.

3.3. Comparison to tetrabenzoporphyrin (TBP)

To further confirm the dehydrocyclization reaction, TBP was deposited directly onto each surface and studied at room temperature and after incremental annealing steps to 710 K (Fig. 5). HREELS spectra of the TBP on Cu(100) and Ag(111) are shown in Table 2 for comparison with OEP. TBP had the same primary C—H bending feature at 735 cm^{-1} as well as similar out-of-plane porphyrin features at 425 and 625 cm^{-1}, but was different from the annealed OEP in the 800–2000 cm^{-1} region. In particular, the feature at 941 cm^{-1} is absent in the surface-formed TBP (OEP annealed to 710 K). This vibrational mode can be correlated to a two-up-two-down C—H bending mode that exists when all four hydrogen are present [66]. Thus, this mode is not present after molecular symmetry is changed through further hydrogen loss. Instead, other C—H bending modes are observed between

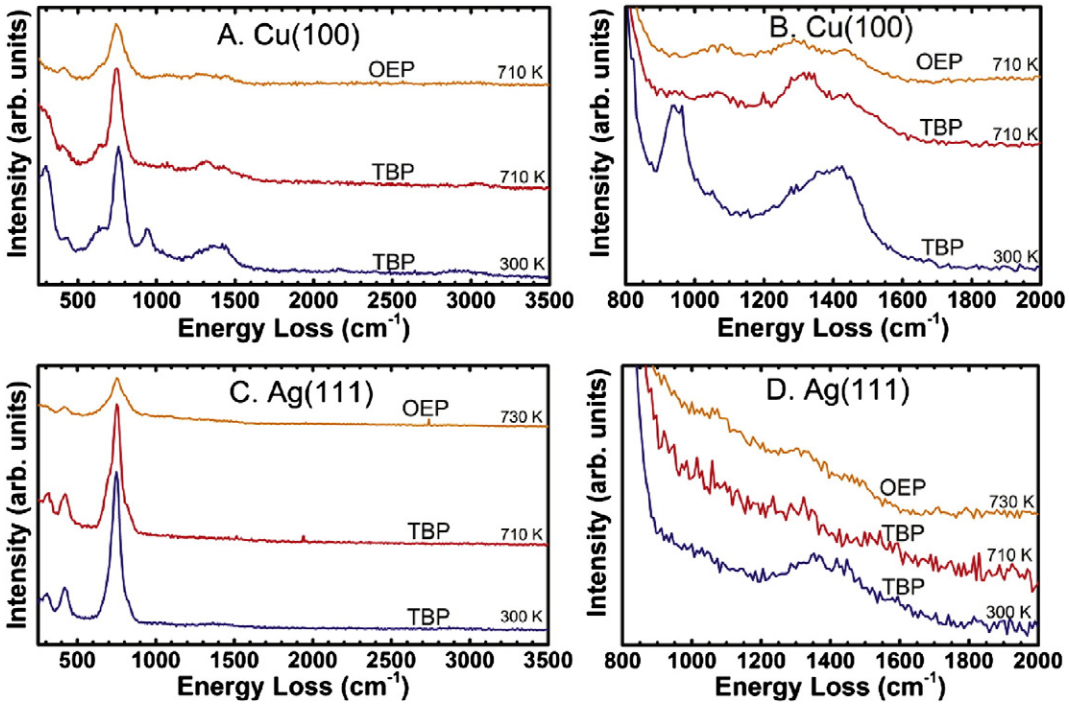

Fig. 5. (A, B) Spectra of TBP and OEP before and after an annealing cycle on the Cu(100) surface. (C, D) Spectra of TBP and OEP before and after an annealing cycle on the Ag(111) surface. (B, D) Close-up spectra showing the in-plane stretch region. (B) is a 3.8× magnification of (A) and (D) is an 11.75× magnification of (C). Selected annealing temperatures are shown here; the spectra for incremental annealing steps of TBP on Cu(100) and Ag(111) can be found in Figs. S6 and S7, respectively.

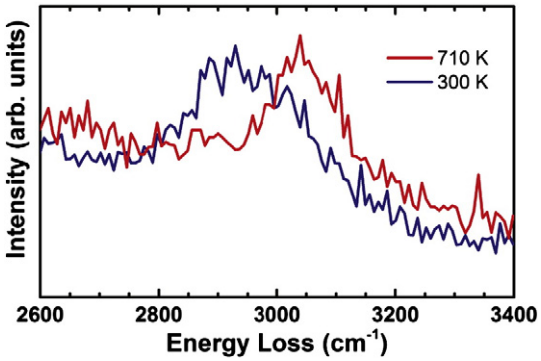

Fig. 6. HREEL spectra of the C—H stretching region for TBP on Cu(100) before (red) and after annealing to 710 K (blue). The peak area after annealing decreased by 25% indicating four hydrogen loss per molecule. The loss of peak area to the lower energy end of the peak indicates that the more weakly bound aryl hydrogen was likely the ones lost.

735 cm^{-1} and 1000 cm^{-1}. Evidence for the dehydrogenation of TBP is that the C—H peak at 3000 cm^{-1} decreases, the feature at 941 cm^{-1} decreases, and there are changes to the 800–2000 cm^{-1} region to match the annealed OEP peaks. The hydrogens that are lost are likely aryl hydrogens (red carbons in Scheme 1) as the 3000 cm^{-1} peak loses intensity on the low energy side (Fig. S6C), consistent with prior studies of phthalocyanines [83,87–90]. The stronger porphyrin methine C—H bonds (green carbons in Scheme 1) are expected to remain intact. The peaks at 1080 and 1430 cm^{-1} remain unchanged with annealing as these are in-plane porphyrin C—C stretches that do not involve carbons in the benzo groups.

Interestingly, the aryl dehydrogenation of TBP occurs at a lower temperature than the dehydrocyclization on either surface. Aryl dehydrogenation of TBP occurred on Cu(100) at 480 K (Fig. S6) and at 500 K on Ag(111) (Fig. S7), compared to dehydrocyclization of OEP at 500 K on Cu(100) and at 600 K on Ag(111). The TBP C—H stretching peak area decreases by 25% (Fig. 6) after annealing at 710 K, indicating loss of four aryl hydrogens per molecule. The C—H bond cleavage could result in several possible chemical configurations of the porphyrin: the TBP carbon could form a bond to the underlying surface, a covalent TBP-TBP linkage could form between neighboring molecules [90], or a TBP-Cu-TPB linkage could form *via* a Cu adatom [87]. STM imaging after annealing of the TBP (Fig. 3C and D) shows some TBP molecules close to each other, but does not provide evidence for extensive TBP linking as was observed through coupling reactions of structurally similar phthalocyanine [90]. Thus, dehydrogenation leading to C-surface bonding may be the most likely model. The dehydrocyclization on Ag(111) yielded similar STM results where molecules are neighboring each other, but again no clear evidence for intermolecular linkage has been detected (Fig. 3C and D).

4. Conclusion

HREEL spectroscopy and STM provide evidence for the dehydrocyclization of the peripheral ethyl units of OEP on Cu(100) and Ag(111) surfaces. While smaller alkane functionalized species would desorb before this reaction takes place, OEP has sufficient stability against thermal desorption for the reaction at 500 and 610 K on Cu(100) and Ag(111), respectively. The dehydrocyclized product then undergoes an additional dehydrogenation step of its benzo aryl hydrogens. This aryl dehydrogenation was also found to occur when TBP is deposited and annealed to 480 K or 500 K on Cu(100) or Ag(111), respectively. The dehydrocyclized OEP and aryl dehydrogenated TBP have very similar spectral features and both are likely forming surface bonds. Metallation of the porphyrin ring, tested by deposition of Pt-OEP or self-metallation on the Cu surface, did not have any effect on the dehydrocyclization temperature. Reaction steps such as these are important considerations in the ongoing development of more sophisticated functional organic architectures at surfaces and in advancing our understanding of surface catalysis.

Acknowledgements

The authors acknowledge the support for this work from the Chemical Sciences, Geosciences and Biosciences Division, Office of Basic Energy Sciences, Office of Science, U.S. Department of Energy, Grant DE-FG02-12ER16351. The authors also thank Mike Hosek and Dave Sprinkle of the IU Physics Department and the Mechanical Instrument Services group of the IU Chemistry Department for the technical development and support.

Appendix A. Supplementary data

Supplementary data to this article can be found online at http://dx.doi.org/10.1016/j.susc.2016.06.013.

References

[1] H. Imahori, Giant multiporphyrin arrays as artificial light-harvesting antennas, J. Phys. Chem. B 108 (2004) 6130–6143.
[2] H. Klauk, Organic Electronics: Materials, Manufacturing, and Applications, John Wiley & Sons, Weinheim, 2006.
[3] I. Mochida, K. Suetsugu, H. Fujitsu, K. Takeshita, Enhanced catalytic activity of cobalt tetraphenylporphyrin on titanium dioxide by evacuation at elevated temperatures for intensifying the complex-support interaction, J. Phys. Chem. 87 (1983) 1524–1529.
[4] J.M. Gottfried, Surface chemistry of porphyrins and phthalocyanines, Surf. Sci. Rep. 70 (2015) 259–379.
[5] Y. Matsuo, Y. Sato, T. Niinomi, I. Soga, H. Tanaka, E. Nakamura, Columnar structure in bulk heterojunction in solution-processable three-layered p-i-n organic photovoltaic devices using tetrabenzoporphyrin precursor and Silylmethyl[60]fullerene, J. Am. Chem. Soc. 131 (2009) 16048–16050.
[6] P. Douglas, K. Eaton, Response characteristics of thin film oxygen sensors, Pt and Pd octaethylporphyrins in polymer films, Sensors Actuators B Chem. 82 (2002) 200–208.
[7] S. Aramaki, Y. Sakai, N. Ono, Solution-processible organic semiconductor for transistor applications: tetrabenzoporphyrin, Appl. Phys. Lett. 84 (2004) 2085–2087.
[8] S. Mohnani, D. Bonifazi, Supramolecular architectures of porphyrins on surfaces: the structural evolution from 1D to 2D to 3D to devices, Coord. Chem. Rev. 254 (2010) 2342–2362.
[9] L. Grill, M. Dyer, L. Lafferentz, M. Persson, M.V. Peters, S. Hecht, Nano-architectures by covalent assembly of molecular building blocks, Nat. Nanotechnol. 2 (2007) 687–691.
[10] Y. Li, J. Xiao, T.E. Shubina, M. Chen, Z. Shi, M. Schmid, H.P. Steinruck, J.M. Gottfried, N. Lin, Coordination and metalation bifunctionality of Cu with 5,10,15,20-tetra(4-pyridyl)porphyrin: toward a mixed-valence two-dimensional coordination network, J. Am. Chem. Soc. 134 (2012) 6401–6408.
[11] S. Berner, M. De Wild, L. Ramoino, S. Ivan, A. Baratoff, H.-J. Güntherodt, H. Suzuki, D. Schlettwein, T. Jung, Adsorption and two-dimensional phases of a large polar molecule: sub-phthalocyanine on Ag(111), Phys. Rev. B 68 (2003) 115410.
[12] S.B. Lei, C. Wang, S.X. Yin, H.N. Wang, F. Xi, H.W. Liu, B. Xu, L.J. Wan, C.L. Bai, Hydrogen bonded 2D network porphyrins, J. Phys. Chem. B 105 (2001) 3.
[13] J. Otsuki, STM studies on porphyrins, Coord. Chem. Rev. 254 (2010) 2311–2341.
[14] K.S. Mali, K. Lava, K. Binnemans, S. De Feyter, Hydrogen bonding versus van der Waals interactions: competitive influence of noncovalent interactions on 2D self-assembly at the liquid–solid interface, Chem. Eur. J. 16 (2010) 14447–14458.
[15] X. Qiu, C. Wang, Q. Zeng, B. Xu, S. Yin, H. Wang, S. Xu, C. Bai, Alkane-assisted adsorption and assembly of phthalocyanines and porphyrins, J. Am. Chem. Soc. 122 (2000) 5550–5556.
[16] B.M. Weckhuysen, R.A. Schoonheydt, Alkane dehydrogenation over supported chromium oxide catalysts, Catal. Today 51 (1999) 223–232.
[17] J.J.H.B. Sattler, J. Ruiz-Martinez, E. Santillan-Jimenez, B.M. Weckhuysen, Catalytic dehydrogenation of light alkanes on metals and metal oxides, Chem. Rev. 114 (2014) 10613–10653.
[18] D. Burtron, Alkane dehydrocyclization mechanism, Catal. Today 53 (1999) 443–516.
[19] C. Hansch, The dehydrocyclization reaction, Chem. Rev. 53 (1953) 353–396.
[20] J. Choi, A.H. MacArthur, M. Brookhart, A.S. Goldman, Dehydrogenation and related reactions catalyzed by iridium pincer complexes, Chem. Rev. 111 (2011) 1761–1779.
[21] A. Friedrich, M. Drees, S. Schneider, Ruthenium-catalyzed dimethylamineborane dehydrogenation: stepwise metal-centered dehydrocyclization, Chem. Eur. J. 15 (2009) 10339–10342.
[22] R.E. Jentoft, M. Tsapatsis, M.E. Davis, B.C. Gates, Platinum clusters supported in zeolite LTL: influence of catalyst morphology on performance inn-hexane reforming, J. Catal. 179 (1998) 565–580.

[23] W. Li, S.Y. Yu, G.D. Meitzner, E. Iglesia, Structure and properties of cobalt-exchanged H-ZSM5 catalysts for dehydrogenation and dehydrocyclization of alkanes, J. Phys. Chem. B 105 (2001) 1176–1184.
[24] G.L. Price, V. Kanazirev, K.M. Dooley, V.I. Hart, On the mechanism of propane dehydrocyclization over cation-containing, proton-poor MFI zeolite, J. Catal. 173 (1998) 17–27.
[25] A.V. Teplyakov, A.B. Gurevich, E.R. Garland, B.E. Bent, J.G. Chen, Mechanism of dehydrocyclization of 1-hexene to benzene on Cu3Pt(111): identification of 1,3,5-hexatriene as reaction intermediate, Langmuir 14 (1998) 1337–1344.
[26] H. He, A.T. Mathauser, A.V. Teplyakov, Self-limiting heterogeneous reactions: bifunctional hydrocarbon on a bimetallic alloy surface, J. Phys. Chem. B 104 (2000) 12306–12314.
[27] J.G. Chen, B. Frühberger, J. Eng Jr., B.E. Bent, Controlling surface reactivities of transition metals by carbide formation, J. Mol. Catal. A Chem. 131 (1998) 285–299.
[28] S. Tjandra, F. Zaera, A surface science study of the hydrogenation and dehydrogenation steps in the interconversion of C6 cyclic hydrocarbons on Ni(100), J. Catal. 164 (1996) 82–93.
[29] A. Mathauser, A. Teplyakov, Naphthalene formation on Cu3Pt(111): dehydrocyclization of 4-phenyl-1-butene, Catal. Lett. 73 (2001) 207–210.
[30] A.V. Teplyakov, B.E. Bent, Mechanism of dehydrocyclization of 1-hexene to benzene on Cu3Pt(111), J. Phys. Chem. B 101 (1997) 9052–9059.
[31] M. Yang, G.A. Somorjai, Adsorption and reactions of C6 hydrocarbons at high pressures on Pt(111) single-crystal surfaces studied by sum frequency generation vibrational spectroscopy: mechanisms of isomerization and dehydrocyclization of n-hexane, J. Am. Chem. Soc. 126 (2004) 7698–7708.
[32] M. Yang, G.A. Somorjai, Evidence for cyclohexyl as a reactive surface intermediate during high-pressure cyclohexane catalytic reactions on Pt(111) by sum frequency generation vibrational spectroscopy, J. Am. Chem. Soc. 125 (2003) 11131–11135.
[33] S. Tjandra, F. Zaera, Thermal chemistry of 1,6-diiodohexane on Ni(100) single-crystal surfaces: mimicking cyclization reactions, J. Phys. Chem. A 103 (1999) 2312–2320.
[34] N. Vasquez Jr., R.J. Madix, Reactivity of unsaturated linear C6 hydrocarbons on Pd(111) and H(D)/Pd(111), J. Catal. 178 (1998) 234–252.
[35] O.E. Finlayson, J.K.A. Clarke, J.J. Rooney, Mechanisms of 1,5-dehydrocyclisation and isomerisation of alkanes on iridium, rhodium, palladium and platinum films, J. Chem. Soc. Faraday Trans. 80 (1984) 191–209.
[36] G.A. Somorjai, R.W. Joyner, B. Lang, The reactivity of low index [(111) and (100)] and stepped platinum single crystal surfaces, Proc. R. Soc. A 331 (1972) 335–346.
[37] A. Paul, M.X. Yang, B.E. Bent, Disproportionation and coupling reactions of alkyl iodides on a Au(111) surface, Surf. Sci. 297 (1993) 327–344.
[38] S. Tjandra, F. Zaera, Thermal chemistry of dihalopropanes on Ni(100) single-crystal surfaces: formation of cyclopropane, propene, and propane, J. Phys. Chem. B 101 (1997) 1006–1013.
[39] D. Chrysostomou, A. Chou, F. Zaera, Thermal chemistry of C3 metallacycles on Pt(111) surfaces, J. Phys. Chem. B 105 (2001) 5968–5978.
[40] A.V. Teplyakov, A.B. Gurevich, M.X. Yang, B.E. Bent, J.G. Chen, NEXAFS and TPD studies of molecular adsorption of hydrocarbons on Cu(100): segmental correlations with the heats of adsorption, Surf. Sci. 396 (1998) 340–348.
[41] A.V. Teplyakov, B.E. Bent, J. Eng Jr., J.G. Chen, Vibrational mode-softening of alkanes on clean and modified Cu and Mo surfaces: absence of a simple correlation with thermal desorption temperatures, Surf. Sci. 399 (1998) L342–L350.
[42] S.L. Tait, Z. Dohnálek, C.T. Campbell, B.D. Kay, n-alkanes on MgO(100). II. Chain length dependence of kinetic desorption parameters for small n-alkanes, J. Chem. Phys. 122 (2005) 164708.
[43] B.A. Sexton, A.E. Hughes, A comparison of weak molecular adsorption of organic molecules on clean copper and platinum surfaces, Surf. Sci. 140 (1984) 227–248.
[44] W. Wei, W.X. Huang, J.M. White, Adsorption of styrene on Ag(111), Surf. Sci. 572 (2004) 401–408.
[45] A. Santra, J. Cowell, R. Lambert, Ultra-selective epoxidation of styrene on pure Cu{111} and the effects of Cs promotion, Catal. Lett. 67 (2000) 87–91.
[46] Y. Sohn, W. Wei, J.M. White, Phenylacetylene on Cu(111): adsorption geometry, interfacial electronic structures and thermal chemistry, J. Phys. Chem. C 111 (2007) 5101–5110.
[47] Y. Sohn, Wei, J.M. White, 1-Phenyl-1-propyne on Cu(111): TOFMS TPD, XPS, UPS, and 2PPE studies, Langmuir 23 (2007) 12185–12191.
[48] W.X. Huang, J.M. White, Growth and orientation of naphthalene films on Ag(111), J. Phys. Chem. B 108 (2004) 5060–5065.
[49] W. Zhao, W. Wei, J.M. White, Two-photon photoemission spectroscopy: naphthalene on Cu(111), Surf. Sci. 547 (2003) 374–384.
[50] A.S. Russell, J.J. Stokes, Role of surface area in dehydrocyclization catalysis, Ind. Eng. Chem. 38 (1946) 1071–1074.
[51] M. Laatikainen, K. Vahteristo, S. Saukkonen, M. Lindström, Kinetics of n-butylbenzene dehydrocyclization over chromia–alumina, Ind. Eng. Chem. Res. 35 (1996) 2103–2109.
[52] M. Roeckert, M. Franke, Q. Tariq, S. Ditze, M. Stark, P. Uffinger, D. Wechsler, U. Singh, J. Xiao, H. Marbach, H.-P. Steinrueck, O. Lytken, Coverage- and temperature-dependent metalation and dehydrogenation of tetraphenylporphyrin on Cu(111), Chem. Eur. J. 20 (2014) 8948–8953.
[53] M. Roeckert, M. Franke, Q. Tariq, D. Lungerich, N. Jux, M. Stark, A. Kaftan, S. Ditze, H. Marbach, M. Laurin, J. Libuda, H.-P. Steinrueck, O. Lytken, Insights in reaction mechanistics: isotopic exchange during the metalation of deuterated tetraphenyl-21,23*D*-porphyrin on Cu(111), J. Phys. Chem. C 118 (2014) 26729–26736.
[54] M. Treier, C.A. Pignedoli, T. Laino, R. Rieger, K. Müllen, D. Passerone, R. Fasel, Surface-assisted cyclodehydrogenation provides a synthetic route towards easily processable and chemically tailored nanographenes, Nat. Chem. 3 (2011) 61–67.
[55] K. Weiss, G. Beernink, F. Dötz, A. Birkner, K. Müllen, C.H. Wöll, Template-mediated synthesis of polycyclic aromatic hydrocarbons: cyclodehydrogenation and planarization of a hexaphenylbenzene derivative at a copper surface, Angew. Chem. Int. Ed. 38 (1999) 3748–3752.
[56] K. Amsharov, N. Abdurakhmanova, S. Stepanow, S. Rauschenbach, M. Jansen, K. Kern, Towards the isomer-specific synthesis of higher fullerenes and buckybowls by the surface-catalyzed cyclodehydrogenation of aromatic precursors, Angew. Chem. Int. Ed. 122 (2010) 9392–9396.
[57] J. Mendez, M.F. Lopez, J.A. Martin-Gago, On-surface synthesis of cyclic organic molecules, Chem. Soc. Rev. 40 (2011) 4578–4590.
[58] B.W. Heinrich, G. Ahmadi, V.L. Müller, L. Braun, J.I. Pascual, K.J. Franke, Change of the magnetic coupling of a metal–organic complex with the substrate by a stepwise ligand reaction, Nano Lett. 13 (2013) 4840–4843.
[59] D. van Vörden, M. Lange, M. Schmuck, J. Schaffert, M.C. Cottin, C.A. Bobisch, R. Möller, Communication: substrate induced dehydrogenation: transformation of octa-ethyl-porphyrin into tetra-benzo-porphyrin, J. Chem. Phys. 138 (2013) 211102.
[60] B. Cirera, N. Giménez-Agulló, J. Björk, F. Martínez-Peña, A. Martin-Jimenez, J. Rodriguez-Fernandez, A.M. Pizarro, R. Otero, J.M. Gallego, P. Ballester, Thermal selectivity of intermolecular versus intramolecular reactions on surfaces, Nat. Commun. 7 (2016).
[61] S. Stepanow, T. Strunskus, M. Lingenfelder, A. Dmitriev, H. Spillmann, N. Lin, J.V. Barth, C. Wöll, K. Kern, Deprotonation-driven phase transformations in terephthalic acid self-assembly on Cu(100), J. Phys. Chem. B 108 (2004) 19392–19397.
[62] S.L. Tait, Y. Wang, G. Costantini, N. Lin, A. Baraldi, F. Esch, L. Petaccia, S. Lizzit, K. Kern, Metal-organic coordination interactions in Fe-terephthalic acid networks on Cu(100), J. Am. Chem. Soc. 130 (2008) 2108–2113.
[63] Y. Ge, H. Adler, A. Theertham, L.L. Kesmodel, S.L. Tait, Adsorption and bonding of first layer and bi-layer terephthalic acid on the Cu(100) surface by high-resolution electron energy loss spectroscopy, Langmuir 26 (2010) 16325–16329.
[64] I. Horcas, R. Fernandez, J.M. Gomez-Rodriguez, J. Colchero, J. Gomez-Herrero, A.M. Baro, WSXM: a software for scanning probe microscopy and a tool for nanotechnology, Rev. Sci. Instrum. 78 (2007) 013705.
[65] H. Ogoshi, N. Masai, Z. Yoshida, J. Takemoto, K. Nakamoto, The infrared spectra of metallooctaethyl porphyrins, Bull. Chem. Soc. Jpn. 44 (1971) 3.
[66] A.M. Botelho do Rego, A.M. Ferraria, M.R. Vilar, Grafting of cobaltic protoporphyrin IX on semiconductors toward sensing devices: vibrational and electronic high-resolution electron energy loss spectroscopy and X-ray photoelectron spectroscopy study, J. Phys. Chem. C 117 (2013) 22298–22306.
[67] L. Scudiero, D. Barlow, K.W. Hipps, Scanning tunneling microscopy, orbital-mediated tunneling spectroscopy, and ultraviolet photoelectron spectroscopy of nickel(II) octaethylporphyrin deposited from vapor, J. Phys. Chem. B 106 (2002) 8.
[68] DFT was performed in spartan with gas phase OEP molecules. A B3LYP 6-31G* level of computation was utilized. The out of plane vibrational modes were found to be at 334 cm^{-1} and 450 cm^{-1}.
[69] Y. Bai, F. Buchner, I. Kellner, M. Schmid, F. Vollnhals, H.-P. Steinrück, H. Marbach, J.M. Gottfried, Adsorption of cobalt (II) octaethylporphyrin and 2H-octaethylporphyrin on Ag (111): new insight into the surface coordinative bond, New J. Phys. 11 (2009) 125004.
[70] F. Buchner, J. Xiao, E. Zillner, M. Chen, M. Röckert, S. Ditze, M. Stark, H.-P. Steinrück, J.M. Gottfried, H. Marbach, Diffusion, rotation, and surface chemical bond of individual 2H-tetraphenylporphyrin molecules on Cu(111), J. Phys. Chem. C 115 (2011) 24172–24177.
[71] H. Ibach, D.L. Mills, Electron Energy Loss Spectroscopy and Surface Vibrations, Academic Press, London, 1982.
[72] F. Thomas, N. Chen, L. Ford, R. Masel, Vibrational/HREELS, UV/HREELS, and temperature-programmed desorption of benzene and hydrogen on (2× 1) Pt (110), Surf. Sci. 486 (2001) 1–8.
[73] G. Waddill, L. Kesmodel, Benzene chemisorption on palladium surfaces. I. High-resolution electron-energy-loss vibrational spectra and structural models, Phys. Rev. B 31 (1985) 4940.
[74] P. Avouris, J. Demuth, Electronic excitations of benzene, pyridine, and pyrazine adsorbed on Ag(111), J. Chem. Phys. 75 (1981) 4783–4794.
[75] D. Huntley, S. Jordan, F. Grimm, Adsorption and thermal decomposition of benzene on nickel (110) studied by chemical, spectroscopic, and computational methods, J. Phys. Chem. 96 (1992) 1409–1417.
[76] R. González-Moreno, C. Sánchez-Sánchez, M. Trelka, R. Otero, A. Cossaro, A. Verdini, L. Floreano, M. Ruiz-Bermejo, A. García-Lekue, J.A. Martín-Gago, C. Rogero, Following the metalation process of protoporphyrin IX with metal substrate atoms at room temperature, J. Phys. Chem. C 115 (2011) 6849–6854.
[77] J. Nowakowski, C. Wackerlin, J. Girovsky, D. Siewert, T.A. Jung, N. Ballav, Porphyrin metalation providing an example of a redox reaction facilitated by a surface reconstruction, Chem. Commun. 49 (2013) 2347–2349.
[78] P. Borghetti, G. Di Santo, C. Castellarin-Cudia, M. Fanetti, L. Sangaletti, E. Magnano, F. Bondino, A. Goldoni, Adsorption geometry, conformation, and electronic structure of 2H-octaethylporphyrin on Ag(111) and Fe metalation in ultra high vacuum, J. Chem. Phys. 138 (2013) 144702.
[79] J.M. Auerhammer, M. Knupfer, H. Peisert, J. Fink, The copper phthalocyanine/Au(100) interface studied using high resolution electron energy-loss spectroscopy, Surf. Sci. 506 (2002) 6.
[80] E. Salomon, T. Angot, N. Papageorgiou, J.M. Layet, Self-assembled monolayer of tin-phthalocyanine on InSb(001)-(4 × 2)/c(8 × 2), Surf. Sci. 596 (2005) 74–81.
[81] F. Roth, A. König, R. Kraus, M. Grobosch, T. Kroll, M. Knupfer, Probing the molecular orbitals of FePc near the chemical potential using electron energy-loss spectroscopy, Eur. Phys. J. B 74 (2010) 339–344.

[82] P. Amsalem, L. Giovanelli, J. Themlin, T. Angot, Electronic and vibrational properties at the ZnPc/Ag(110) interface, Phys. Rev. B 79 (2009) 235426.
[83] S. Haq, F. Hanke, M.S. Dyer, M. Persson, P. Iavicoli, D.B. Amabilino, R. Raval, Clean coupling of unfunctionalized porphyrins at surfaces to give highly oriented organometallic oligomers, J. Am. Chem. Soc. 133 (2011) 12031–12039.
[84] M. Losurdo, M.M. Giangregorio, P. Capezzuto, G. Bruno, Graphene CVD growth on copper and nickel: role of hydrogen in kinetics and structure, Phys. Chem. Chem. Phys. 13 (2011) 20836–20843.
[85] R.J. Koch, T. Haensel, S.I.U. Ahmed, T. Seyller, J.A. Schaefer, HREELS study of graphene formed on hexagonal silicon carbide, Phys. Status Solidi C 7 (2010) 394–397.
[86] A.M. Shikin, G.V. Prudnikova, V.K. Adamchuk, Surface intercalation of gold underneath a graphite monolayer on Ni(111) studied by angle-resolved photoemission and high-resolution electron-energy-loss spectroscopy, Phys. Rev. B 62 (2000) 7.
[87] S. Haq, F. Hanke, J. Sharp, M. Persson, D.B. Amabilino, R. Raval, Versatile bottom-up construction of diverse macromolecules on a surface observed by scanning tunneling microscopy, ACS Nano 8 (2014) 8856–8870.
[88] W. Auwarter, A. Weber-Bargioni, S. Brink, A. Riemann, A. Schiffrin, M. Ruben, J.V. Barth, Controlled metalation of self-assembled porphyrin nanoarrays in two dimensions, Chem. Phys. Chem. 8 (2007) 250–254.
[89] A. Wiengarten, K. Seufert, W. Auwarter, D. Ecija, K. Diller, F. Allegretti, F. Bischoff, S. Fischer, D.A. Duncan, A.C. Papageorgiou, F. Klappenberger, R.G. Acres, T.H. Ngo, J.V. Barth, Surface-assisted dehydrogenative homocoupling of porphine molecules, J. Am. Chem. Soc. 136 (2014) 9346–9354.
[90] Q. Sun, C. Zhang, L. Cai, L. Xie, Q. Tan, W. Xu, On-surface formation of two-dimensional polymer via direct C—H activation of metal phthalocyanine, Chem. Commun. 51 (2015) 2836–2839.